Raman scheme to measure the quantum statistics of an atom laser beam

A. S. Bradley,[1,2] M. K. Olsen,[1,2] S. A. Haine,[1,3] and J. J. Hope[1,3]

[1]*Australian Research Council Centre of Excellence for Quantum-Atom Optics, Queensland 4072, Australia*
[2]*School of Physical Sciences, University of Queensland, Brisbane, Queensland 4072, Australia*
[3]*Department of Physics, Australian National University, Canberra, Australia*

We propose and analyze a scheme for measuring the quadrature statistics of an atom laser beam using extant optical homodyning and Raman atom laser techniques. Reversal of the normal Raman atom laser outcoupling scheme is used to map the quantum statistics of an *incoupled* atomic beam to an optical probe beam. A multimode model of the spatial propagation dynamics shows that the Raman incoupler gives a clear signal of de Broglie wave quadrature squeezing for both pulsed and continuous inputs. Finally, we show that experimental realizations of the scheme may be tested with existing methods via intensity correlation measurements.

I. INTRODUCTION

Quantum-atom optics [1–3], the study of quantum properties of matter waves, is a rapidly developing subfield of ultracold atomic physics. Recent experimental progress includes measurements of intensity correlations of noncondensed ^{20}Ne [4], Hanbury Brown–Twiss correlations [5,6], fermion pairing correlations [7], spatial correlations of density fluctuations [8], and sub-Poissonian number fluctuations [9]. Despite the advances in atom detection techniques that have made such measurements possible, the information available is essentially restricted to intensity correlations. As is well known in quantum optics, probing quantum states generated by nonlinear interactions requires controllable phase-sensitive detection. Optical quadratures, analogous to the momentum and position of a particle, are measured via homodyne detection [10,11]. This technique has been used to demonstrate optical squeezing [12,13], the Einstein-Podolsky-Rosen (EPR) paradox for photons [14], and continuous-variable teleportation [15]. Although interference measurements [16], including those using heterodyne-type techniques [17], as well as intensity correlation and tomographic measurements [18] have been performed with bosonic matter waves, a practical scheme to realize matter wave homodyne detection has not yet been demonstrated.

Proposed methods for producing matter waves in highly nonclassical states include utilizing the nonlinear atomic interactions to create correlated pairs of atoms via either molecular down-conversion [19], spin exchange collisions [20,21], or transferring the quantum state of a nonclassical electromagnetic field to a propagating atomic field [22–24]. In some of these schemes, it has been demonstrated that continuous-variable entanglement can be generated between spatially separated atomic beams [19,23] or between an atomic beam and an optical beam [25], which can be used to perform tests of quantum nonlocality with massive particles. Although schemes for atomic homodyne measurements have been proposed these are confined to trapped Bose-Einstein condensates (BECs) [26–28], whereas quadrature measurements on free atomic fields will be necessary to observe the effects mentioned above.

In this work, we propose a scheme for dynamically transferring quantum information from a propagating atom laser beam to an optical beam, allowing indirect measurement of de Broglie wave quadrature variances via optical homodyning. The strength of this scheme is that it does not require a mode-matched atomic local oscillator, which would be very difficult to achieve experimentally. By analogy with optical quadratures, $\hat{X}(\theta) = \hat{a}e^{-i\theta} + \hat{a}^{\dagger}e^{i\theta}$, we may use atomic field operators to define atomic quadratures [19], and the scheme that we analyze here is designed to measure the quadratures of a propagating atomic beam. It involves a reversal of the successful Raman atom laser output coupling scheme [29,30], a variant of which has previously been proposed as a mechanism for transferring states of a nonclassical optical field to the outgoing atomic beam [23,25,31]. As we will show, a two-photon Raman transition allows the atom laser beam to be incoupled [32] to a large trapped condensate, with highly efficient transfer of the atomic statistics to an outgoing optical field.

II. SYSTEM AND EQUATIONS OF MOTION

The scheme (Fig. 1) consists of a trapped condensate and an incoming atom laser beam of the same species. The internal Raman energy level configuration allows for stimulated transitions between the trapped and untrapped fields. These transitions are stimulated by two optical fields, one of which is intense (control) and denoted by its Rabi frequency $\Omega(x,t)$, while the other is much weaker (probe) and denoted by the field operator $\hat{E}(x,t)$. We perform our analysis using a one-dimensional model, described by the Hamiltonian $\mathcal{H} = \mathcal{H}_{\text{atom}} + \mathcal{H}_{\text{int}} + \mathcal{H}_{\text{light}}$, with

$$\mathcal{H}_{\text{atom}} = \sum_{j=1}^{3} \int dx\, \hat{\psi}_j^{\dagger}(x) H_j \hat{\psi}_j(x), \qquad (1)$$

$$\mathcal{H}_{\text{int}} = \hbar \int dx [\hat{\psi}_2(x)\hat{\psi}_3^{\dagger}(x)\Omega(x,t) + \text{H.c.}]$$
$$+ \hbar g_{13} \int dx [\hat{E}(x)\hat{\psi}_1(x)\hat{\psi}_3^{\dagger}(x) + \text{H.c.}], \qquad (2)$$
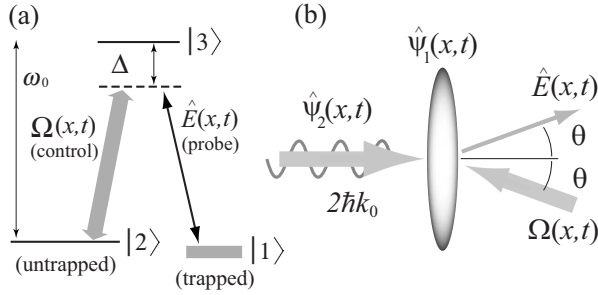
FIG. 1. Schematic of a Raman atom laser incoupler. (a) Λ configuration of three-level atoms. An untrapped beam of $|2\rangle$ atoms is coupled to a trapped state $|1\rangle$ via a Raman transition. The two optical fields are a weak probe beam [annihilation operator $\hat{E}(x,t)$], and a control beam [$\Omega(x,t)$], modeled by a classical field. The transition is detuned from the intermediate state by Δ. Wide lines represent highly occupied states. (b) Spatial configuration of the Raman atom laser system. Beam atoms [field operator $\hat{\psi}_2(x,t)$] reach the condensate [$\hat{\psi}_1(x,t)$] with momentum $2\hbar k_0$, which is transferred during incoupling by absorption and emission of light quanta with momenta $\mp \hbar k_0$ along the propagation axis.

$$\mathcal{H}_{\text{light}} = \int dx\, \hat{E}^{\dagger}(x)pc\hat{E}(x), \tag{3}$$

where $H_1 = -\hbar^2 \partial_x^2/2m + V_1(x)$, $H_2 = -\hbar^2 \partial_x^2/2m + V_2(x)$, $H_3 = -\hbar^2 \partial_x^2/2m + \hbar\omega_0 + V_3(x)$, m is the atomic mass, and the V_j represent both linear (trapping for $\hat{\psi}_1$) and nonlinear (scattering) potentials. ω_0 is the excitation frequency of the upper level $|3\rangle$. The optical control field is $\Omega(x,t) = \Omega_{23} e^{i[k_0 x - (\omega_0 - \Delta)t]}$ where Ω_{23} is the Rabi frequency for the $|2\rangle \rightarrow |3\rangle$ transition. $\hat{\psi}_1(x)$, $\hat{\psi}_2(x)$, $\hat{\psi}_3(x)$, and $\hat{E}(x)$ are the annihilation operators for the condensate mode (internal state $|1\rangle$), signal beam ($|2\rangle$), excited-state atoms ($|3\rangle$), and probe beam photons, respectively, satisfying the usual bosonic commutation relations, $[\hat{\psi}_i(x), \hat{\psi}_j^{\dagger}(x')] = \delta_{ij}\delta(x-x')$ and $[\hat{E}(x), \hat{E}^{\dagger}(x')] = \delta(x-x')$. $\mathcal{H}_{\text{light}}$ depends on the speed of light in vacuum (c) and the momentum operator $p = -i\hbar\partial_x$. The coupling coefficient is $g_{13} = (d_{13}/\hbar)\sqrt{\hbar\omega_k/2\epsilon_0 A}$, where d_{13} is the electric dipole moment for the $|1\rangle \rightarrow |2\rangle$ transition, $\hbar\omega_k = kc$, and A is the cross-sectional area of the coupling region (we use A corresponding to a control laser beam waist of 100 μm). We neglect interatomic interactions on the basis that the atomic beam is dilute and the process will take place over a time short enough that any phase diffusion effects will be minimal. We now introduce the rotating-frame fields $\tilde{\psi}_3(x) = \hat{\psi}_3(x)e^{i(\omega_0-\Delta)t}$ and $\tilde{E}(x) = \hat{E}(x)e^{i(\omega_0-\Delta)t}$ and adiabatically eliminate the weakly occupied intermediate state [25,31] $\tilde{\psi}_3(x) \rightarrow -(\Omega_{23}/\Delta)e^{ik_0 x}\hat{\psi}_2(x) - (g_{13}/\Delta)\tilde{E}(x)\hat{\psi}_1(x)$. We approximate the highly occupied condensate as a coherent state, $\hat{\psi}_1(x,t) = \phi(x,t) \equiv \langle \hat{\psi}_1(x,t) \rangle$, while allowing the occupation and the spatial shape to change. To simplify notation we set $\hat{\psi}_2 \equiv \hat{\psi}$ to arrive at the equations of motion

$$i\dot{\hat{\psi}}(x) = H_a\hat{\psi}(x) - \Omega_C(x)e^{-ik_0 x}\tilde{E}(x), \tag{4}$$

$$i\dot{\tilde{E}}(x) = H_b\tilde{E}(x) - \Omega_C^*(x)e^{ik_0 x}\hat{\psi}(x), \tag{5}$$

$$i\dot{\phi}(x) = H_\phi\phi(x) - \frac{g_{13}\Omega_{23}}{\Delta}e^{ik_0 x}\langle \hat{E}^{\dagger}(x)\hat{\psi}(x)\rangle \tag{6}$$

with $H_a = -\hbar\partial_x^2/2m - |\Omega_{23}|^2/\Delta$, $H_b = -ic\partial_x - |\phi(x)|^2(g_{13})^2/\Delta + \Delta - \omega_0$, $H_\phi = -\hbar\partial_x^2/2m + V_1(x)/\hbar - \langle \hat{E}^{\dagger}(x)\hat{E}(x)\rangle(g_{13})^2/\Delta$, and $\Omega_C(x) = \phi(x)\Omega_{23}^* g_{13}/\Delta$. As shown in Ref. [31], equations of this type can be efficiently solved to give all relevant observables.

III. SIMULATIONS

We now consider two special cases to determine the accuracy and limitations of the scheme: an atom laser pulse and a continuous atom laser beam. To understand the transfer of quantum information in the system, we must define mode-matched quadratures [19] which characterize the probe light and the atomic signal. We define a mode of the atomic ($\nu = \psi$) or optical ($\nu = E$) field, $L_\nu(x,t)$, and the operators $\hat{a}_\nu = \int_{x_1^\nu}^{x_2^\nu} dx\, L_\nu^*(x,t)\hat{\nu}(x,t)$, with the normalization $\int_{x_1^\nu}^{x_2^\nu} dx\, L_\nu^*(x,t)L_\nu(x,t) = 1$, satisfying $[\hat{a}_\nu, \hat{a}_{\nu'}^{\dagger}] = \delta_{\nu\nu'}$. The mode-matched quadratures $\hat{X}_\nu^+ = \hat{a}_\nu + \hat{a}_\nu^{\dagger}$, $\hat{X}_\nu^- = i(\hat{a}_\nu^{\dagger} - \hat{a}_\nu)$ have commutator $[\hat{X}_\nu^+, \hat{X}_{\nu'}^-] = 2i\delta_{\nu\nu'}$ and uncertainty relation $V(\hat{X}_\nu^+)V(\hat{X}_\nu^-) \geq 1$.

A. Atom laser pulse

We first consider an amplitude-squeezed atomic pulse propagating into the interaction region, with a weak optical probe field (linear intensity 1.9×10^{-7} m^{-1}) incident on the condensate. This defines the transverse mode of the emitted probe photons. The atomic, pump, and probe wave vectors are $2k_0$, $-k_0$, and k_0, respectively, with $k_0 = 8 \times 10^6$ m^{-1}, giving an atom laser beam velocity of $v_{\text{atom}} = 1.1$ cm s^{-1}. The input pulse $L_\psi(x,0)$ is a Gaussian of width $\sigma_x = 100$ μm containing $n_0 = 5 \times 10^3$ atoms. We use $N_0 = 10^6$ condensate atoms, trapped with potential $V_1(x) = m\omega_t^2 x^2/2$, with frequency $\omega_t = 5$ Hz. In all cases we operate at the optimal efficiency point for the signal so that the ratio of the condensate width to the mean beam velocity is tuned to one quarter of a Rabi cycle, $T_{\text{Rabi}} \approx 4\sqrt{\hbar/m\omega_t}(m/2\hbar k_0)$ [25]. The input atom laser pulse is modeled as an X_ψ^+-squeezed minimum uncertainty state with $V(\hat{X}_\psi^{\pm}) = e^{\mp 2r}$, where r (≥ 0) parametrizes the degree of squeezing. Figure 2(a) shows the field intensities when the pulse is almost half incoupled. When the probe is initially in the vacuum state there is no outcoupling and the incoupling is almost perfectly efficient. In the presence of a continuous weak probe (shown here) some outcoupling also occurs. The probe quadrature variances for both cases are plotted in Fig. 2(b). The incident probe light and the outcoupling dynamics have a negligible effect on the quadrature signal when compared with the vacuum probe case (identical on this scale). The squeezing of the input pulse is transmitted to the probe, allowing the quadrature statistics of the atom laser to be read out via optical homodyne detection of the
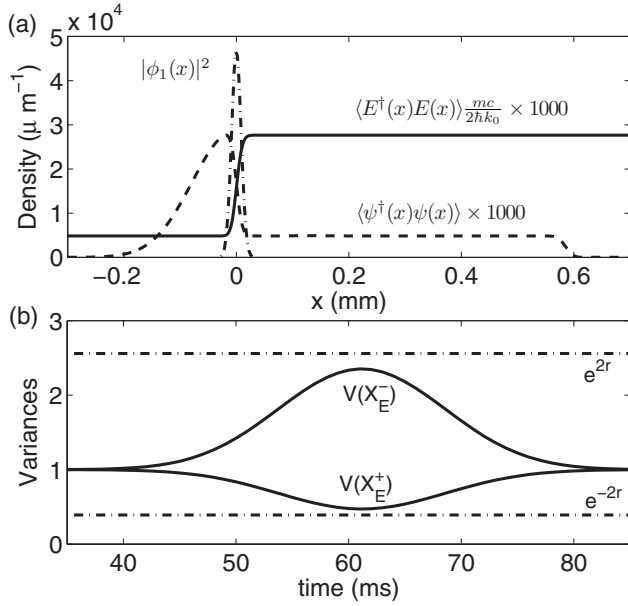
FIG. 2. Incoupling an atom laser pulse. (a) Squeezed atomic pulse (4 dB in the X^+ quadrature, dashed line) of $n_0 = 5 \times 10^3$ atoms initially centered at $x = -600$ μm, with momentum wave vector $2k_0$, is coupled into the condensate (chain line). The probe field (solid line) has peak intensity occurring at $t = 54$ ms shown here, which is when the maximum of the pulse is centered on the condensate. The atom pulse and optical probe are magnified by factors of 1000 and $1000 mc/2\hbar k_0$ to plot them on the condensate scale. (b) Time development of the probe quadratures. A value of less than 1 demonstrates quadrature squeezing and the chain lines give the atomic variances.

probe light. This result demonstrates a limitation of pulsed dynamics: the squeezed quadrature of the probe shows less squeezing than the input atomic pulse. While the effect is not always large, it is significant for the chosen scenario because the spatial extent of the squeezed pulse is much larger than the condensate. The signal degrades because different parts of the same atomic wave packet are subject to different Rabi frequencies while traveling across the interaction region.

B. Atom laser beam

We now show that for continuous, essentially monochromatic, squeezed atom laser input [31] the spatial effects are removed and the scheme efficiently maps the physical variances of the beam to the probe. Figure 3 shows the Raman incoupling dynamics. The system now consists of a squeezed atom laser beam in a nearly monochromatic state (wave vector $2k_0$) which enters from the left. The atoms are incoupled
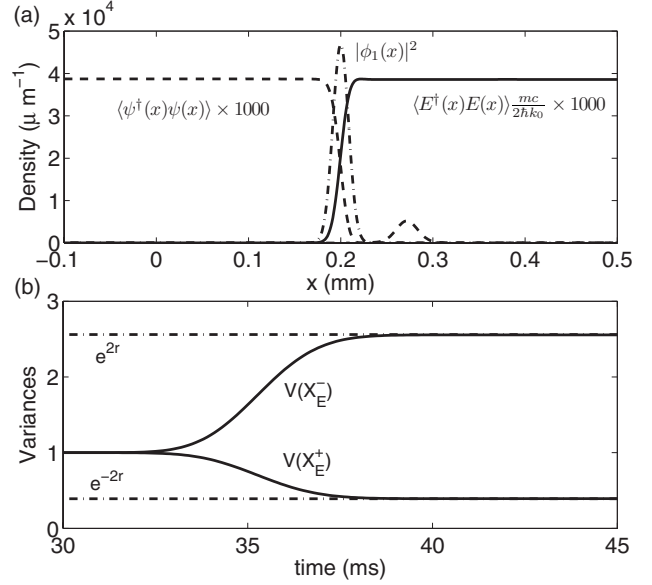

FIG. 3. Incoupling a continuous atom laser beam. (a) Snapshot of the atomic beam (dashed line), condensate (chain line), and probe (solid line) during incoupling. (b) Development of the optical quadratures (solid lines) as the front of the atom laser beam crosses the interaction region. The zero of the time axis is arbitrary. The chain lines show the variances of the 4 dB squeezed atomic beam.

via the reversed Raman scheme, emitting probe photons. Once the front of the beam crosses the interaction region the system is approximately in a steady state (except for the gradual transfer of atoms into the trapped condensate), with a constant probe output. We see that the quadrature variances of the emitted probe light reach steady-state values very close to the atom laser variances.

IV. ATOM COUNTING STATISTICS

To provide a test of the scheme that could be carried out independently, we now show analytically that the local $g^{(2)}$ can be extracted from the probe field with high efficiency. In fact we derive a more general result relating $g_\nu^{(2)}(x,x,t)$ $\equiv \langle \hat{\nu}^\dagger(x,t)\hat{\nu}^\dagger(x,t)\hat{\nu}(x,t)\hat{\nu}(x,t)\rangle / \langle \hat{\nu}^\dagger(x,t)\hat{\nu}(x,t)\rangle^2$ to the initial state of the atom laser beam and the probe field. Since the system is linear we may introduce a linear ansatz for the field operators $\hat{\nu}(x,t) = f_\nu(x,t)\hat{a}_0 + h_\nu(x,t)\hat{b}_0$, where the evolution of f_ν, h_ν gives the field time development and the initial states are given by the single-mode bosonic operators $\hat{a}_0$ (atoms) and $\hat{b}_0$ [33]. For the systems we consider, one of $\langle \hat{b}_0 \rangle$ or $\langle \hat{a}_0 \rangle$ is zero, and the atom laser beam and optical probe are initially uncorrelated. We immediately find

$$g_\nu^{(2)}(x,x,t) = \frac{|f_\nu(x,t)|^4\langle \hat{a}_0^\dagger\hat{a}_0^\dagger\hat{a}_0\hat{a}_0\rangle + |h_\nu(x,t)|^4\langle \hat{b}_0^\dagger\hat{b}_0^\dagger\hat{b}_0\hat{b}_0\rangle + 4|f_\nu(x,t)|^2|h_\nu(x,t)|^2\langle \hat{a}_0^\dagger\hat{a}_0\rangle\langle \hat{b}_0^\dagger\hat{b}_0\rangle}{|f_\nu(x,t)|^4\langle \hat{a}_0^\dagger\hat{a}_0\rangle^2 + |h_\nu(x,t)|^4\langle \hat{b}_0^\dagger\hat{b}_0\rangle^2 + 2|f_\nu(x,t)|^2|h_\nu(x,t)|^2\langle \hat{a}_0^\dagger\hat{a}_0\rangle\langle \hat{b}_0^\dagger\hat{b}_0\rangle},$$

(7)

where the field density $\langle \hat{\nu}(x,t)\hat{\nu}(x,t)\rangle$ is nonzero. The case of special interest here is when the optical probe is initially in the vacuum state, so that $h_\nu(x,t) \equiv h_\nu(x,0) = 0$ and $g_\nu^{(2)}(x,x,t) = \langle \hat{a}_0^\dagger \hat{a}_0^\dagger \hat{a}_0 \hat{a}_0 \rangle / \langle \hat{a}_0^\dagger \hat{a}_0 \rangle^2$, where defined. This demonstrates that $g_\psi^{(2)}(x,x,t)$ is mapped to the emitted probe light under Raman incoupling evolution. This correlation can be directly measured [9], potentially providing a test of the scheme that does not require quadrature information.

DISCUSSION AND CONCLUSIONS

Apart from the stability of the lasers used, the main sources of possible signal degradation are spontaneous emission losses and phase noise due to atomic collisions. The effect of spontaneous emission can be estimated from the spontaneous emission rate for a transition with energy $\omega_0 = k_0 c$ radiating into a continuum, $\gamma_{sp} = k_0^3 |d_{13}|^2 / 3\pi\hbar\epsilon_0$. The total spontaneous loss during the incoupling is then $L_{sp} = \gamma_{sp} \int dx \int dt \langle \hat{\psi}_3^\dagger(x,t)\hat{\psi}_3(x,t)\rangle$. Using the adiabatically eliminated expression for the excited state $\langle \hat{\psi}_3^\dagger(x,t)\hat{\psi}_3(x,t)\rangle \approx \langle \hat{\psi}_2^\dagger(x,t)\hat{\psi}_2(x,t)\rangle (\Omega_{23}/\Delta)^2$, and the fact that each excited atom on average remains excited for time $T_{Rabi}/4$, we have $L_{sp} \lesssim \gamma_{sp} \bar{N}_3 T_{Rabi}/4$, where $\bar{N}_3$ is the total number of excited-state atoms transferred per squeezed mode. For the incoupling process to remain coherent, we require $L_{sp}/\bar{N}_3 \ll 1$, and upon integration over the entire input pulse for our parameters we find $L_{sp}/\bar{N}_3 \approx 0.04$. We can now estimate the effect on the signal phenomenologically using a beam splitter that mixes the signal and vacuum with reflectivity η (≈ 0.04 here). The probe variances then become $V(\hat{X}_E^\pm) = (1-\eta)V(\hat{X}_\psi^\pm) + \eta$, acceptable for small η.

The collisions between the incoming and the trapped atoms will have two undesired effects. First, there will be a mean-field shift to the condensate energy which will tend to rotate the quadrature phases. This will be negligible when the number of incoupled atoms is much smaller than the condensate occupation. This is likely to be the case in any practical realization of the scheme. The second effect will be that of phase diffusion of the beam, which to a first approximation will cause an increase in the variance of the phase quadrature. We may consider this effect by noting that the velocity transferred to ^{23}Na by the Raman transition can be up to 6 cm/s, with up to 1.2 cm/s for ^{87}Rb. Using a single-mode expression for the phase diffusion [34] and the parameters of

Fig. 2, we find that ^{23}Na can travel up to 3 mm and ^{87}Rb up to 600 μm in their respective coherence times. As this is larger than the diameter of the present condensates, the effect will be small. Another issue that will arise is that the probe beam will be emitted into a narrow cone rather than as a well-collimated beam. This can be simply overcome using linear optical elements.

Another important consideration is the role of condensate phase in our scheme. Although for simplicity we have treated the BEC as a coherent state, in practice this does not pose a significant restriction. A reasonable model for a BEC is a coherent state with an *a priori* random phase. It is clear from Eqs. (4)–(6) that the dynamics are sensitive to the phase of $\phi(x)$. However, from our numerical simulations we have found that changing the initial phase of the condensate simply rotates the phase space quadratures of the output optical field, so that for any given experimental run the spontaneously chosen phase will be automatically compensated for when all angles are scanned over during optical homodyne detection.

Finally, we address the effect of a thermal component on the phase stability of the condensate during incoupling. Since phase diffusion is most significant at high temperatures, we use quantum kinetic theory [35]. One immediately finds that during the incoupling interaction time the phase diffusion is entirely negligible for the condensate parameters we have used here, assuming a temperature of order ~ 100 nK. The decay of the relevant two-time correlation function, namely, $\langle \phi^\dagger(x,t)\phi(x',t')\rangle$ [where $\phi(x,t)$ is the condensate field operator], is typically at the level of one part in 10^8 during the incoupling time.

In conclusion, we have shown that a Raman incoupler scheme may be used as a means to measure the quantum statistics of an atom laser by transferring quadrature variances to an optical probe on which standard homodyne measurements may be made. Experimental realization of our proposal would allow access to quantum features of matter fields, including demonstrations of squeezing, entanglement between atomic beams, atom-light entanglement, and the EPR paradox with matter waves, which are not available with other methods.

ACKNOWLEDGMENTS

[1] G. Lenz, P. Meystre, and E. M. Wright, Phys. Rev. Lett. **71**, 3271 (1993).

[2] S. L. Rolston and W. D. Phillips, Nature (London) **416**, 219 (2002).

[3] P. L. Knight, Science **310**, 631 (2005).

[4] M. Yasuda and F. Shimizu, Phys. Rev. Lett. **77**, 3090 (1996).

[5] M. Schellekens *et al.*, Science **310**, 648 (2005).

[6] C.-S. Chuu, F. Schreck, T. P. Meyrath, J. L. Hanssen, G. N. Price, and M. G. Raizen, Phys. Rev. Lett. **95**, 260403 (2005).

[7] M. Greiner, C. A. Regal, J. T. Stewart, and D. S. Jin, Phys. Rev. Lett. **94**, 110401 (2005).

[8] S. Fölling *et al.*, Nature (London) **434**, 481 (2005).

[9] A. Öttl, S. Ritter, M. Köhl, and T. Esslinger, Phys. Rev. Lett. **95**, 090404 (2005).

[10] H. P. Yuen and J. H. Shapiro, in *Coherence and Quantum Optics IV*, edited by L. Mandel and E. Wolf (Plenum, New

York, 1978).

[11] M. J. Collett, R. Loudon, and C. W. Gardiner, J. Mod. Opt. **34**, 881 (1987).

[12] R. E. Slusher, L. W. Hollberg, B. Yurke, J. C. Mertz, and J. F. Valley, Phys. Rev. Lett. **55**, 2409 (1985).

[13] L.-A. Wu, H. J. Kimble, J. L. Hall, and H. Wu, Phys. Rev. Lett. **57**, 2520 (1986).

[14] Z. Y. Ou, S. F. Pereira, H. J. Kimble, and K. C. Peng, Phys. Rev. Lett. **68**, 3663 (1992).

[15] A. Furusawa *et al.*, Science **282**, 706 (1998).

[16] M. R. Andrews *et al.*, Science **275**, 637 (1997).

[17] Z. Hadzibabic *et al.*, Nature (London) **441**, 1118 (2006).

[18] K. L. Moore, S. Gupta, K. W. Murch, and D. M. Stamper-Kurn, Phys. Rev. Lett. **97**, 180410 (2006).

[19] K. V. Kheruntsyan, M. K. Olsen, and P. D. Drummond, Phys. Rev. Lett. **95**, 150405 (2005).

[20] L.-M. Duan, A. Sørensen, J. I. Cirac, and P. Zoller, Phys. Rev. Lett. **85**, 3991 (2000).

[21] H. Pu and P. Meystre, Phys. Rev. Lett. **85**, 3987 (2000).

[22] H. Jing, J.-L. Chen, and M.-L. Ge, Phys. Rev. A **63**, 015601 (2000).

[23] S. A. Haine and J. J. Hope, Phys. Rev. A **72**, 033601 (2005).

[24] M. Fleischhauer and S. Gong, Phys. Rev. Lett. **88**, 070404 (2002).

[25] S. A. Haine, M. K. Olsen, and J. J. Hope, Phys. Rev. Lett. **96**, 133601 (2006).

[26] J. F. Corney and G. J. Milburn, Phys. Rev. A **58**, 2399 (1998).

[27] C. P. Search, Phys. Rev. A **64**, 053606 (2001).

[28] B. R. da Cunha and M. C. de Oliveira, Int. J. Mod. Phys. B **20**, 1671 (2006).

[29] G. M. Moy, J. J. Hope, and C. M. Savage, Phys. Rev. A **55**, 3631 (1997).

[30] E. W. Hagley *et al.*, Science **283**, 1706 (1999).

[31] S. A. Haine and J. J. Hope, Laser Phys. Lett. **2**, 597 (2005).

[32] V. V. Paranjape, P. V. Panat, and S. V. Lawande, Int. J. Mod. Phys. B **17**, 4465 (2003).

[33] This ansatz is used to exactly solve the equations of motion numerically [31], and is introduced here for normally ordered operator averages.

[34] M. J. Steel, M. K. Olsen, L. I. Plimak, P. D. Drummond, S. M. Tan, M. J. Collett, D. F. Walls, and R. Graham, Phys. Rev. A **58**, 4824 (1998).

[35] C. W. Gardiner and P. Zoller, Phys. Rev. A **58**, 536 (1998).